Power-Dependent Characteristics of Spin Current Transfer in Metal Bilayer Devices under High-Power Pulse Excitation

Power-Dependent Characteristics of Spin Current Transfer in Metal Bilayer Devices under High-Power Pulse Excitation

Kenta Nakahashi, Kohei Takaishi, Takayuki Suzuki, Katsuichi Kanemoto

Citation	ACS Applied Materials & Interfaces. 14(18); 21217-21223.
Issue Date	2022-05-11
Published online	2022-04-27
Type	Journal Article
Textversion	Author
Rights	This document is the Accepted Manuscript version of a Published Work that appeared in final form in ACS Applied Materials & Interfaces, copyright © 2022 American Chemical Society after peer review and technical editing by the publisher. To access the final edited and published work see https://doi.org/10.1021/acsami.2c03418.
DOI	10.1021/acsami.2c03418

Nakahashi, K., Takaishi, K., Suzuki, T., & Kanemoto, K. (2022). Power-Dependent Characteristics of Spin Current Transfer in Metal Bilayer Devices under High-Power Pulse Excitation. *ACS Applied Materials & Interfaces.* 14, 21217–21223. https://doi.org/10.1021/acsami.2c03418

Power-Dependent Characteristics of Spin Current Transfer in Metal Bilayer Devices under High-Power Pulse Excitation

*Kenta Nakahashi[1], Kohei Takaishi[1], Takayuki Suzuki[2], Katsuichi Kanemoto[1,3]**

1 *Department of Physics, Graduate School of Science, Osaka City University, 3-3-138 Sugimoto, Sumiyoshi-ku, Osaka 558-8585, Japan.*

2 *JEOL RESONANCE Inc., 3-1-2 Musashino, Akishima, Tokyo 196-8558, Japan.*

3 *Nambu Yoichiro Institute of Theoretical and Experimental Physics (NITEP), Osaka City University, 3-3-138 Sugimoto, Sumiyoshi-ku, Osaka 558-8585, Japan.*

KEYWORDS: Spin current, permalloy/Pt, inverse spin Hall effect, ferromagnetic resonance, pulse excitation

ABSTRACT. The power-dependent transfer characteristics of spin currents generated at the interface of the permalloy/Pt bilayer device have been investigated over a wide power range from a few tens of mW to 396W. We built a high power pulse excitation system for spin pumping,

which achieves large electromotive force (EMF) values of 10mV at 396W excitation through the inverse spin Hall effect (ISHE) and demonstrates that the EMF generation after pulse excitation is very fast. Under strong pulse microwave excitation more than 80 W, the EMF spectrum exhibits an asymmetrical lineshape, which is well reproduced by simulations that take into account the fold-over effect due to the non-linear ferromagnetic resonance excitation. The maximum output power at an external load through spin pumping and ISHE is shown to increase in proportion to the square of the input microwave power (P_{in}) in the power range below 80W. This power generation proportional to P_{in}^2 is unique to spin current-mediated power flow. In the strong excitation regime with the fold-over type EMF spectra, the EMF values of peak magnetic field position are found to increase less linearly due to spectral broadening. This feature can be used for power generation that increases nonlinearly with respect to the input excitation power, where the nonlinearity is adjusted by varying the magnetic field position.

1. Introduction

Understanding the transfer mechanism of spin currents and establishing effective methods of efficient spin current transfer is a very important issue for the field of spin current research. The combination of spin pumping by ferromagnetic resonance (FMR) excitation and inverse spin Hall effect (ISHE) has been widely used as one of the most effective methods to study the propagation process of spin currents in multilayer thin-film devices consisting of ferromagnetic (FM) and non-magnetic (NM) layers.[1-5] The ISHE process generates an electromotive force (EMF) through charge currents converted from spin currents, and the EMF generates electric power. The sequence of processes from the spin pumping to the EMF generation can thus be regarded as transfer and

output processes of spin-excited power, which is of interest to the field of spintronics. However, under normal continuous microwave irradiation of about 100mW for FMR excitation, the EMF induced is typically only a few μV, which is too small to be considered for future application as a spintronics device. Simply increasing the microwave power can make the EMF larger, but it may cause a temperature increase of devices and reduce the magnetization of FM layer. To circumvent the temperature increase, strong excitation by pulsed high power microwaves with short widths could be effective. [6] However, the characteristics of transfer process of spin excitation power under high power short pulse excitation have not been well studied and, therefore, should be fully understood toward future device applications.

It has been reported that the EMF of ISHE increases in proportion to the microwave irradiation power,[6-8] which is important characteristics in understanding the transfer process of spin excitation power. However, most of the power-dependent ISHE experiments have been performed under relatively weak excitation power below 1W, and the characteristics of ISHE under much stronger microwave irradiation have not been sufficiently explored. In particular, it is known that, under strong microwave excitation, non-linear responses of FMR signals are often observed with distortion of the lineshape called a foldover effect.[9-13] ISHE experiments in the regime of such nonlinear FMR responses are not only interesting from a physical properties point of view, but also important for a comprehensive understanding of the transfer process of spin excitation power over a wide power range, and should be fully explored.

In this article, the characteristics of ISHE under strong microwave irradiation are investigated for the metal bilayer device consisting of permalloy (Py) and Pt layers employed as a prototype of the most studied bilayer devices. The microwave power is increased even to about 400W, and such high power microwave is pulsed to reduce the effect of device heating. The pulsed ISHE

techniques allow us to measure the ISHE-induced EMF in the time domain, demonstrating that the response of the EMF signal is very fast. We show that a fold-over like lineshape is obtained from the EMF-spectra under strong microwave excitation, suggesting that a non-linear response is included in the FMR excitation for spin pumping. The output power via EMF generated at the Pt layer is found to increase in proportion to the square of incident microwave power, which arises from the characteristics of the power propagation via spin current. Under strong excitation which induces the fold-over lineshapes, the incident power dependence of the output power varies due to the broadening of the FMR spectrum. These characterizations of the output power provide a basis for understanding the transfer process of the spin excitation power and are important for future applications.

2. Experiments

The device fabricated was the Py/Pt bilayer on a quartz substrate. The quartz substrate was first subjected to ultrasonic cleaning in the order of distilled water, acetone, and 2-propanol for 15 minutes each, and then UV-ozone cleaning for 10 minutes. A 5 nm-thick Pt layer was formed by vacuum evaporation (13mm×2.5mm) on the cleaned quartz substrate. A permalloy (Ni 78% and Fe 22%) layer (15nm-thickness) was formed by vacuum evaporation (6mm×2.5mm) on the Pt layer. The two Ag electrode lines to pick up EMF signals were produced by vacuum evaporation using a shadow mask on the Pt surface (20nm thickness) so that the upper and lower electrode lines were parallel to each other to reduce signals from spin rectification effects such as anisotropic magnetoresistance and anomalous Hall effect signals which may broaden the FMR line width.[14] The device was connected to a thin conducting wire with silver paste and then inserted into a glass cell for EMF measurements and sealed in a nitrogen-filled glove box.

The EMF signals of the Py/Pt device were measured for a device arrangement where the static magnetic field was parallel to the two Ag electrode lines on the device surface. The EMF measurement was performed using a partially modified conventional X band ESR spectrometer (JES-FE1XG, JEOL Ltd.) with a rectangular TE_{102} microwave cavity (ES-PCX1, JEOL RESONANCE Inc.). For the EMF measurements under the incident microwave power less than 1W, the EMF was measured by a lock-in technique (SR-830, SRS) synchronized with the amplitude modulation of microwave (1.0 kHz). The voltage values by the lock-in measurements were corrected to the peak-to-peak output values. In the EMF measurements with high-intensity microwave pulse, the output from the microwave unit was shaped into a pulse waveform by a double balanced mixer (typical pulse width 500ns) and the pulse output amplified by the traveling wave tube amplifier (TWTA) was irradiated to the device. A gate trigger for driving the TWTA was controlled by the OPENCORE NMR spectrometer.[15-17] In the measurements of microwave absorption power, the microwave power emitted from a light guide window on the front side of the cavity was measured by a detection diode (75KA50, Anritsu) connected with a pick-up antenna.[14] All measurements were performed at room temperature.

3. Results and discussion

3.1. Non-linear characteristics of ISHE-induced EMF

In typical magnetic resonance experiments using pulsed microwaves, short pulses with a width less than 100ns are often adopted to observe time-dependent phonomena.[18] In such conventional transient measurements with short pulses, a cavity with a low Q-value driven by over coupling with the waveguide is generally used to excite a wide frequency domain. However, such small Q-value cavities reduce the irradiation intensity of samples, resulting in a decrease in signal intensity.

In the present study for the Py/Pt bilayer device, the EMF via ISHE is obtained from the thin Pt layer (5nm) when the pulse FMR excitation occurs at the Py layer. Then the propagation of the spin current in the thin Pt film should be very fast: for instance, the propagation could end in 5 ns even at a small velocity of about 1 m/s. Thus, the time difference between the pulse excitation and EMF generation should be very short, less than 1 ns, meaning that the propagation process is difficult to observe unless the pulse width is considerably shortened. Therefore, we did not adopt a low Q-cavity equipment. Instead, we constructed a system which can irradiate strong microwave pulses with the width of 500 ns under almost critical coupled condition using high Q-valued cavity (ca. 1100). It enables more effective spin excitation and allows us to obtain larger EMF values

Figure 1 compares the two EMF spectra of the Py/Pt bilayer obtained from lock-in measurements under excitation power of 162mW with 50% duty cycle and from direct measurements with a digital oscilloscope under pulsed microwave irradiation of 80W. The latter measurement was performed by recording EMF voltages during pulse excitation continuously while sweeping magnetic field. The lock-in spectrum is symmetrical and can be fitted with a Lorentzian line shape of the half-width at half-maximum (HWHM) of 2.89 mT, but the spectrum at 80W exhibits a slightly distorted line shape, which is discussed later.

Figure 2(a) shows the results of time-resolved EMF measurements at the EMF peak magnetic field under the 396W-incident pulse. The time response waveform of EMF showing a 4.0 mV-peak is obtained directly from the oscilloscope without a preamplifier for the input (or load) resistance of R_L =50Ω due to the use of the high Q-value cavity. This panel also shows the waveform of the irradiated microwave pulse, and its time-response is similar to that of the EMF, indicating that no delay is observed in the EMF response after pulse excitation. Similar results were reported from a previous study using high-power pulsed microwaves, showing EMF with no delay relative to the

pulse.[6] In the experiments under high power microwave irradiation, one must be careful about the effect of heat generation on the EMF. The time response of EMF with no delay means that the EMF rapidly reaches equilibrium during the pulse. Thus, even if the EMF includes the effect of heat generation, it is limited to the case where heat dissipation takes place immediately. We found that the EMF value after the pulse excitation slightly fluctuates as the repetition frequency of pulse is increased, which could be due to the increase of temperature by the pulse excitation. However, such fluctuation was almost negligible at the frequency of 500 Hz used in this study and the obtained EMF was stable for at least one hour of pulse repetition experiments with high power. From these results, we regard that the effect of heating on EMF is negligibly small in these pulse measurements. Figure 2b compares the time-response waveforms of EMF between the measurement at R_L=50 and 1MΩ. The waveform for R_L= 1MΩ shows only a slight delay around the rise and fall of the signal compared to that R_L=50Ω. The resistance of the Pt electrode that generates the EMF was 84.5Ω, and, considering the impedance difference between the Pt resistance and R_L, the larger mismatch at R_L= 1MΩ is presumed to cause the slight delay. Even with R_L= 1MΩ, equilibrium is rapidly achieved within the pulse width of 500 ns, and its intensity reaches as high as 10.2 mV, which was achieved by using the high-Q cavity.

Figure 3a shows the irradiation power dependence of the pulsed EMF spectra measured under R_L= 1MΩ at the time when the EMF reaches the equilibrium value. The peak intensity of the spectra increases with increasing the pulse power, and the EMF spectra exhibit asymmetric line shape with a peak shifted to the high field side. It has been observed that the FMR lineshape of Py is distorted under strong excitation.[10-12] In the case of EMF spectrum, since the EMF is obtained through several processes such as the FMR-absorption, spin injection into the Pt layer, and the

conversion from spin current to charge current by ISHE, it should thus be confirmed whether the observed EMF lineshape is determined only by the FMR absorption lineshape or not.

In magnetic resonance measurements using a microwave cavity under strong pulse irradiation as typically employed in electron spin resonance (ESR), because of strong power reflection from the cavity and leakage through the circulator, direct observation of microwave absorption signal of a sample during the pulse irradiation is usually not possible. In fact, the absorption signals can be observed only when the cavity reflection is sufficiently small such that the absorption signals remain even after the pulse is turned off.[19,20] In addition, when the linewidth of the FMR or ESR signal is large, the absorption signal decays faster, making it even more difficult to detect the absorption signal. In the present case, the linewidth of the Py signal is too large to be detected by such pulse measurements, meaning that the FMR signal of Py under pulsed irradiation cannot be obtained by conventional pulse magnetic resonance methods. We here apply an antenna-probe method to measure FMR absorption spectra under intense pulse excitation. The antenna probe system, consisting of an antenna to pick up microwave and a detection diode, directly measures the microwave power emitted from the front window of a microwave cavity, enabling observation of the microwave absorption spectra by lock-in techniques as demonstrated for the Py/Pt device under quasi-continuous microwave irradiation below 200mW at 50% duty cycle.[14] However, the high power excitation system using TWTA must operate under low duty cycles (typically < 2 %), in which case conventional lock-in techniques cannot provide a significant signal. To overcome such difficulties, absorption spectra by the antenna probe under high-power pulses were measured by gating the antenna response signal according to the pulse width with a boxcar integrator and amplifying the gated response.

Figure 3b shows the FMR spectrum during the pulse excitation under 396W irradiation obtained from the antenna probe measurement, exhibiting an asymmetric spectrum with a peak tilted toward the high magnetic field side. The same figure also shows the EMF spectrum obtained simultaneously with the antenna measurement. The two spectral shapes are similar except for the baseline fluctuation included only in the antenna measurement. This similarity of the spectra demonstrates that the anisotropic EMF spectrum under strong pulse excitation is due to anisotropic lineshape by FMR absorption.

It has been reported that anisotropic lineshape appears in the FMR-spectrum of Py with increasing the irradiation microwave power.[10-12] The anisotropy is due to a nonlinear FMR response that occurs due to large-angle precession caused by strong excitation and results in the resonance peak shift increased with the microwave power, which is often called a fold-over effect and has also been reported on yttrium-iron-garnet (YIG).[13,21-24] In fact, for Py, Khivintsev *et al*. showed that the fold-over-type lineshape appears depending on the magnitude ratio of the static and microwave magnetic fields,[11] and Guo *et al*. showed that the direction of the peak shift in the fold-over spectra changes from lower to higher field sides depending on the aspect ratio of the sample width and length.[12] The spectrum of the fold-over FMR can be described by the following equation:[10,12]

$$L = \frac{A}{(H - H_0 + aL)^2 + \Delta H^2} \quad (1)$$

where L is the FMR intensity, H the magnetic field, H_0 the resonance center, ΔH the linewidth, A the factor proportional to the squared field of microwave, and a the deviation factor of the resonance center proportional to the magnetization. We can here obtain the spectral lineshape by calculating the solution of Eq. (1) as a function of magnetic field. Actually, as shown in Fig. 3c, we succeeded in reproducing the spectrum under 396W-excitation by the calculation. This good

agreement demonstrates that the origin of the EMF-spectrum is indeed due to fold-over FMR absorption, which also confirms that the nonlinear FMR response is included in the EMF-generation process under the strong microwave irradiation.

3.2. Power dependence of spin current-mediated power transfer

In considering the application of spin current-based devices, the EMF and power mediated by spin current should be enhanced, for which exploring the nature and underlying physics of the irradiation power dependence of ISHE-based EMF is important. We here address the excitation power dependence of EMF over a wide power range including that under strong pulse excitation.

We first build a model to analyze the power flow mediated by spin currents. In Fig. 2(b), the steady-state EMF values obtained at R_L=50Ω and 1MΩ under 396 W pulse irradiation were 4.0mV and 10.2mW, respectively. The difference of these values is discussed to build the model. The charge current converted from the spin currents in the Pt layer is consumed by the resistance of the Pt layer and the input resistance (external load) as Joule heat. We expect that the converted current is distributed into the two current components at the Pt layer and the external load defined by $J_{pt} = V_{emf} / R_{pt}$ and $J_L = V_{emf} / R_L$, respectively, where V_{emf} is the EMF measured, and R_{pt} the resistance of Pt layer. We also assume that the total charge current converted from the spin current is constant regardless of R_L. This model is equivalent to assuming a parallel circuit consisting of the two resistance components at the Pt layer and the external load shown in Fig. 4(a) and similar to the model proposed by Rogdakis *et al*..[25] From the assumption of the constant total currents J_c (= J_L + J_{pt}) regardless of R_L, we can calculate V_{emf} at R_L=50Ω ($V_{emf,50}$) by the relation of $V_{emf,1M}(1+10^{-6}R_{pt})/(1+R_{pt}/50)$, where $V_{emf,1M}$ is V_{emf} at R_L=1MΩ. We find that, using simply the resistance of Pt measured between the EMF measurement terminals (84.5Ω) for R_{pt}, $V_{emf,50}$ is

calculated to be -3.80mV using $V_{emf,1M}$= -10.2mV, which is close to the actual $V_{emf,50}$ value (Table 1). Also J_c (= V_{emf} ($1/R_L$+$1/R_{pt}$)) calculated from $V_{emf,50}$ and $V_{emf,1M}$ are shown to be nearly the same for R_L = 50Ω and 1MΩ in Table 1, indicating the validity of the model.

To further confirm the validity of the model, the R_L-dependence of V_{emf} measured in the R_L range of 50Ω to 1MΩ under the 162mW irradiation for the Py/Pt device is compared with the prediction calculated from the relation of $V_{emf,1M}(1+10^{-6}R_{pt})/(1+R_{pt}/R_L)$ (Fig. 4(b)). The prediction curve calculated as a function of R_L reproduces well the R_L-dependence of V_{emf}, confirming the validity of the model. We emphasize that the R_L-dependence of all circuit elements such as V_{emf}, J_L and J_{pt} can be predicted only by measuring simple parameters of V_{emf} at a certain R_L (e.g. 1MΩ) and a resistance between the EMF measurement terminals. Figure 4(b) also shows that J_c calculated from V_{emf} is nearly constant in the R_L range, demonstrating that J_c can be regarded as truly constant regardless of R_L-magnitude.

The model with the equivalent circuit in Fig. 4a enables us to evaluate the effect of R_L on the output power at the external load. Focusing on the fact that output power is generated by irradiating microwave, the power generation can be treated in the same way as in the case of solar cells, where the maximum output is calculated from the current/voltage characteristics measured between output terminals under light irradiation. In the present case, the current/voltage characteristic corresponds to the relation between J_L and V_{emf}, which can be calculated from the R_L dependence of V_{emf} as J_L=V_{emf}/R_L. The output power at the load P_{out} is thus given by

$$P_{\mathrm{out}} = J_{\mathrm{L}}V_{\mathrm{emf}} = \frac{V_{emf}^2}{R_{\mathrm{L}}} = \frac{J_c^2}{R_{\mathrm{L}}\left(\frac{1}{R_{\mathrm{L}}}+\frac{1}{R_{\mathrm{pt}}}\right)^2} \quad . \quad (2)$$

When changing R_L, since J_c is constant from the equivalent circuit model confirmed above, P_{out} is expected to have the maximum value P_{out}^{max} = (1/4)$J_c^2R_{pt}$ when R_L= R_{pt} from the fourth side of Eq.(2). In fact, Figure 4(c) shows that the R_L-dependence of P_{out} calculated from the R_L-

dependence of V_{emf} under the 162mW microwave irradiation has a peak around $R_L = R_{pt}$ and can be reproduced by the fit using the fourth side of Eq.(2).

Since J_L is zero when $R_L \rightarrow \infty$, J_c is calculated from the V_{emf}-value at $R_L \rightarrow \infty$ (V_∞) as $J_c = V_\infty / R_{pt}$. P_{out}^{max} can thus be estimated by substituting the V_{emf}-value at R_L=1MΩ for V_∞. We here define the maximum power output efficiency per irradiation power as follows:

$$\eta_{in}^{max} = {P_{out}^{max}}/{P_{in}} = {V_\infty^2}/{(4R_{pt}P_{in})} \quad (3)$$

Comparing this efficiency between for P_{in} =162 mW and 80 W, the efficiencies are 1.2×10^{-12} for 162mW and 6.6×10^{-10} for 80W, respectively, using V_∞= 8.27μV and 4.22mV substituted by the V_{emf}-values measured under R_L= 1MΩ. Surprisingly, η_{in}^{max} under 80 W is about 550 times greater than that under 162mW as summarized in Fig. 5(a). This finding suggests that the conversion efficiency is enhanced by increasing the irradiation power.

To consider the reason of the power-dependent efficiency, we focus on the property reported previously that the magnitude of FMR-induced EMF is proportional to the microwave irradiation power, [6-8] which could also occur even under strong pulse irradiation.[6] Actually, a nearly linear relation of V_∞ versus P_{in} was obtained under the irradiation microwave power region of P_{in}< 200mW as discussed later. Furthermore, the ratio of V_∞/P_{in} at 162mW to that at 80W was 0.97, confirming a nearly linear relationship between V_∞ and P_{in} including under 80W. Here, assuming $V_\infty = aP_{in}$ with the proportional coefficient a, we obtain the following relation:

$$\eta_{in}^{max} = \frac{(aP_{in})^2}{4P_{in}R_{pt}} = \frac{a^2P_{in}}{4R_{pt}} \propto P_{in} \quad . \quad (4)$$

This relation suggests that η_{in}^{max} increases in proportion to P_{in}. In fact, the increase in η_{in}^{max} under P_{in} =80W against that P_{in} =162 mW (550-fold) is close to the increase in P_{in} (490-fold). Also a

nearly linear relation in η_{in}^{max} versus P_{in} is actually obtained under P_{in}< 200mW (Fig. 5(b)). It is thus confirmed that the power output efficiency is proportional to P_{in}.

This feature of the power conversion efficiency means that if the microwave pulse width for spin pumping is halved and the power is doubled, the output energy obtained through the spin current is twice as large, while the incident pulse energy is the same. Moreover, the increase of η_{in}^{max} depending on P_{in} is actually caused by the increase of the absorption power proportional to P_{in} in the FM layer. In the present experiments, since the efficiency of microwave absorption is very low,[14] increasing the quality-factor of the microwave cavity and optimizing a device structure for efficient microwave absorption can further enhance η_{in}^{max}. Also the transfer efficiency of absorption power from the FM layer to the NM layer can also be enhanced by selecting FM materials that exhibit a large variation of FMR width by addition of a NM layer, or by optimizing the combination of FM and NM materials for efficient spin current transfer. Considering all these, the output efficiency of spin energy through spin currents still could be increased significantly.

We note that the total power provided by J_c generated in the Pt layer and the external load is calculated as $P_{tot} = V_\infty^2(1/R_L + 1/R_{pt}) \propto P_{in}^2$ using the equivalent circuit in Fig. 4a, indicating that P_{tot} is also increased in proportion to P_{in}^2. Therefore, the observed power-dependent features are not limited to the external output, but represent the intrinsic nature of the power conversion process via spin currents. The origin of this feature is here discussed. The number of spins excited by FMR in the Py layer is in proportion to P_{in} and thereby paramagnetic spins in the Pt layer are excited by the FMR-excited spins in proportion to P_{in} (the number of excited spins is n_p). J_s is then formed by a population of the paramagnetic spins and should be proportional to n_p. Assuming that the conversion efficiency from J_s to J_c (the spin Hall angle θ_{sh}) is independent of n_p, the relation of J_c

$\propto P_{in}$ is obtained. Since P_{out} and P_{tot} are in proportion to J_c^2, the two powers are eventually found to increase in proportion to P_{in}^2, explaining also η_{in}^{max} increasing proportional to P_{in}.

The observed P_{in}-dependence can be explained phenomenologically as described above. However, note that, originally, charge current is a quantity that increases in proportion to the squared root of the power. Nonetheless, J_c converted from J_s increases in proportion to P_{in} as long as θ_{sh} is constant regardless of P_{in}. This property of J_s is the origin of the observed P_{in}-dependence of P_{tot}, and it arises from the characteristic of J_s that carries not only angular momentum but also power by a population of excited states. As shown previously, the absorption lineshape and linewidth in the Py/Pt device do not vary with changing P_{in} below 200mW.[14] In this P_{in} range, the fraction of the power injected from the Py layer to the Pt layer by spin pumping (P_{sp}) to P_{in}, corresponding to the linewidth difference between the Py/Pt and Py-only devices divided by the Py-only linewidth,[14] is unlikely to vary in changing P_{in}. In this case, importantly, since J_s is created in proportion to P_{in}, the fraction of P_{tot} within P_{sp} increases in proportion to P_{in} (Figure 5(c)).

P_{sp} is the power excluding the self-relaxation power of Py in the absorption power by the Py layer and can be regarded here as the power reaching the interface with Pt. Figure 5c then means that the portion of the power reaching the interface that is converted to P_{tot} increases in proportion to P_{in}^2. The low η_{in}^{max} values shown above imply that there is much power loss at the interface, but, considering the power conservation law, the increase of P_{tot} in proportion to P_{in}^2 should be supplied by the interface loss power, meaning that the interface power loss can be reduced with increasing P_{in}. Generally, the effect of interface between FM and NM layers on spin current generation is evaluated in terms of the spin-mixing conductance ($g^{\uparrow\downarrow}$). However, since $g^{\uparrow\downarrow}$ is usually defined as a quantity proportional to the difference in FMR linewidth between the FM and FM/NM layers, [26-28] it is proportional to J_s [28-30] (here also P_{sp}), but is unlikely to vary with P_{in} in

the P_{in} range where there is no change in linewidth. Therefore, it should be noted that P_{in}-dependent changes in power transfer at the interface cannot be discussed if the effects of the interface are evaluated only from $g^{\uparrow\downarrow}$. Our findings derived from power-dependent properties of spin currents indicate that the power transfer at the interface should be considered as a power-dependent process.

The aforementioned discussion was made for the results under quasi-continuous microwave irradiation less than 200 mW. The power-dependent properties under pulsed intense excitation are here addressed. As shown in Fig. 3a, under the strong excitation, the peak magnetic field position of the EMF-spectrum shifts to the high field side with increasing P_{in}. Figure 5d shows the plots of the V_{emf} peak intensities against the pulse irradiation power (P_{in}). Unlike the power dependence of V_{emf} below 200 mW, which exhibits a linear relationship as shown in the inset, the V_{emf} peak intensities increase less than linearly with increasing P_{in}. To consider the reason for the less-linear relation, we focus on the V_{emf} spectra in Fig. 3a that become broader as the power increases mainly due to a power-enhanced distortion of the lineshape by the fold-over effect. We consider that the spectral broadening may reduce the peak intensities and thus investigated the P_{in}-dependence of the integrated intensity of the spectrum as in Fig. 5d, showing that the integral intensities exhibit nearly linear P_{in}-dependence. Therefore, when the spectral width broadening is taken into account, a linear increase in V_{emf} proportional to the incident power occurs even under high power pulse irradiation. However, the power-generation proportional to P_{in}^2 cannot occur at fixed magnetic field positions unlike the case in the low power excitation. Instead, V_{emf} at fixed magnetic field positions can exhibit a nonlinear change due to the spectral broadening that varies depending on the field position: for instance, when fixed at the peak position of the 396W-EMF spectrum in Fig. 3a, V_{emf} increases rapidly beyond the linear relation as the power is increased. The non-linear

power generation through fold-over type FMR is expected to be applied for a device whose power generation efficiency can be tuned depending on the magnetic field.

4. Conclusions

We built the high power pulse excitation system for spin pumping and applied it for the Py/Pt device. This system employed a high-Q cavity with critical coupling instead of the conventional low-Q cavity with over-coupling, which enabled excitation with high excitation density. The pulse measurements showed that the transfer of spin excitation power mediated by spin current is very fast and the V_{EMF} induced by high power excitation exceeds 10mV. The high-power spin pumping exhibited asymmetrical EMF-spectra, which were shown to be due to the fold-over effect by non-linear FMR excitation. The conversion, transfer and output processes of the power generated by FMR-pumping were examined for the Py/Pt device. The charge current converted from spin current was shown to be divided into the two currents flowing the Pt layer and the external load, constituting the parallel circuit. The conversion efficiencies of P_{out} and P_{tot} to P_{in} were demonstrated to increase in proportion to P_{in}. These findings mean that the interfacial loss in the generation process of spin current is reduced by increasing P_{in}, indicating the importance of considering the P_{in}-dependence of the interfacial loss in the spin current generation process. In the strong excitation regime with the fold-over type EMF spectra, V_{EMF} was found to be increased less linearly due to the spectral broadening. This feature can be used for power generation increased non-linearly that can be tuned depending on the magnetic field position.

AUTHOR INFORMATION

Corresponding Author

* To whom correspondence should be addressed; E-mail: kkane@osaka-cu.ac.jp

ACKNOWLEDGMENT

This work was supported in part by JSPS KAKENHI Grant (numbers 19K22172 and 21H01906) and by the Osaka City University (OCU) Strategic Research Grant 2021 for basic researches.

REFERENCES

(1) Saitoh, E.; Ueda, M.; Miyajima, H.; Tatara, G. Conversion of spin current into charge current at room temperature: Inverse spin-Hall effect. Applied Physics Letters 2006, 88, 182509.

(2) Sinova, J.; Valenzuela, S. O.; Wunderlich, J.; Back, C. H.; Jungwirth, T. Spin Hall effects. Rev. Modern Phys 2015, 87, 1213-1259.

(3) Iguchi, R.; Saitoh, E. Measurement of Spin Pumping Voltage Separated from Extrinsic Microwave Effects. J. Phys. Soc. Jpn 2017, 86, 011003.

(4) Jin, L. C.; Jia, K. C.; Zhang, D. N.; Liu, B.; Meng, H.; Tang, X. L.; Zhong, Z. Y.; Zhang, H. W. Effect of Interfacial Roughness Spin Scattering on the Spin Current Transport in YIG/NiO/Pt Heterostructures. Acs Appl. Mater. Interfaces 2019, 11, 35458-35467.

(5) Singh, B. B.; Jena, S. K.; Samanta, M.; Biswas, K.; Bedanta, S. High Spin to Charge Conversion Efficiency in Electron Beam-Evaporated Topological Insulator Bi2Se3. Acs Appl. Mater. Interfaces 2020, 12, 53409-53415

(6) Sun, D. L.; van Schooten, K. J.; Kavand, M.; Malissa, H.; Zhang, C.; Groesbeck, M.; Boehme, C.; Vardeny, Z. V. Inverse spin Hall effect from pulsed spin current in organic semiconductors with tunable spin-orbit coupling. Nature Materials 2016, 15, 863-869.

(7) Mosendz, O.; Vlaminck, V.; Pearson, J. E.; Fradin, F. Y.; Bauer, G. E. W.; Bader, S. D.; Hoffmann, A. Detection and quantification of inverse spin Hall effect from spin pumping in permalloy/normal metal bilayers. Phys. Rev. B 2010, 82, 214403.

(8) Jungfleisch, M. B.; Chumak, A. V.; Kehlberger, A.; Lauer, V.; Kim, D. H.; Onbasli, M. C.; Ross, C. A.; Klaui, M.; Hillebrands, B. Thickness and power dependence of the spin-pumping effect in Y3Fe5O12/Pt heterostructures measured by the inverse spin Hall effect. Phys. Rev. B 2015, 91, 134407.

(9) Gui, Y. S.; Wirthmann, A.; Mecking, N.; Hu, C. M. Direct measurement of nonlinear ferromagnetic damping via the intrinsic foldover effect. Phys. Rev. B 2009, 80, 060402(R).

(10) Gui, Y. S.; Wirthmann, A.; Hu, C. M. Foldover ferromagnetic resonance and damping in permalloy microstrips. Phys. Rev. B 2009, 80, 184422.

(11) Khivintsev, Y.; Kuanr, B.; Fal, T. J.; Haftel, M.; Camley, R. E.; Celinski, Z.; Mills, D. L. Nonlinear ferromagnetic resonance in permalloy films: A nonmonotonic power-dependent frequency shift. Phys. Rev. B 2010, 81, 054436.

(12) Guo, F.; Belova, L. M.; McMichael, R. D. Nonlinear ferromagnetic resonance shift in submicron Permalloy ellipses. Phys. Rev. B 2015, 91, 064426.

(13) Zhou, H. G.; Fan, X. L.; Ma, L.; Cui, L.; Jia, C. L.; Zhou, S. M.; Gui, Y. S.; Hu, C. M.; Xue, D. S. Spin pumping in the nonlinear dynamic regime of a Pt/Y3Fe5O12 heterostructure. Appl. Phys. Lett. 2016, 108, 192408.

(14) Nakahashi, K.; Takaishi, K.; Suzuki, T.; Kanemoto, K. Quantifying Power Flow Processes Mediated by Spin Currents. Acs Appl. Electron. Mater. 2021, 3, 1663-1670. Acs Appl. Electron. Mater. 2021, 3, 4254.

(15) Takeda, K. A highly integrated FPGA-based nuclear magnetic resonance spectrometer. Rev. Sci. Instrum. 2007, 78, 033103.

(16) Takeda, K. OPENCORE NMR: Open-source core modules for implementing an integrated FPGA-based NMR spectrometer. Journal of Magnetic Resonance 2008, 192, 218-229.

(17) Takeda, K. Highly Customized NMR Systems Using an Open-Resource, Home-Built Spectrometer. Annual Reports on Nmr Spectroscopy, 2011, 74, 355-393.

(18) Schweiger, A. PULSED ELECTRON-SPIN-RESONANCE SPECTROSCOPY - BASIC PRINCIPLES, TECHNIQUES, AND EXAMPLES OF APPLICATIONS. Angew. Chem. Int. Ed, 1991, 30, 265-292.

(19) Schweiger, A. and Jeschke,G. "Principles of pulse electron paramagnetic resonance" OXFORD (2001).

(20) Goldfarb, D. and Stoll, S. edited, "EPR SPECTROSCOPY, FUNDERMENTALS AND METHODS" WILEY (2018).

(21) Demidov, V. E.; Hansen, U. H.; Demokritov, S. O. Spin-wave eigenmodes of a saturated magnetic square at different precession angles. Phys. Rev. Lett. 2007, 98, 157203.

(22) Gerrits, T.; Krivosik, P.; Schneider, M. L.; Patton, C. E.; Silva, T. J. Direct detection of nonlinear ferromagnetic resonance in thin films by the magneto-optical Kerr effect. Phys. Rev. Lett. 2007, 98, 207602.

(23) Olson, H. M.; Krivosik, P.; Srinivasan, K.; Patton, C. E. Ferromagnetic resonance saturation and second order Suhl spin wave instability processes in thin Permalloy films. J. Appl. Phys. 2007, 102, 023904.

(24) Yan, M.; Vavassori, P.; Leaf, G.; Fradin, F. Y.; Grimsditch, M. Non-linear response of driven spin excitations. J. Magn. Magn. Mater. 2008, 320, 1909-1915.

(25) Rogdakis, K.; Alfert, N.; Srivastava, A.; Robinson, J. W. A.; Blamire, M. G.; Cohen, L. F.; Kurebayashi, H. Electric power transfer in spin-pumping experiments. Appl. Phys. Exp. 2018, 11, 013004.

(26) Tserkovnyak, Y.; Brataas, A.; Bauer, G. E. W.; Halperin, B. I. Nonlocal magnetization dynamics in ferromagnetic heterostructures Rev. Mod. Phys. 2005, 77, 1375-1421.

(27) Cao, R.; Fan, X.; Moriyama,T.; Xiao, J. Q. Nonlinear effective spin-mixing conductance in Pt/$Ni_{80}Fe_{20}$/Pt thin films. J. Appl. Phys. 2009, 105, 07C705.

(28) Mosendz, O. Vlaminck, Pearson, V. J. Fradin, E. F. Y. Bauer, G. E. W. Bader, S. D. Hoffmann, A. Detection and quantification of inverse spin Hall effect from spin pumping in permalloy/normal metal bilayers. Phys. Rev. B 2010, 82, 214403.

(29) Ando, K.; Takahashi, S.; Ieda, J.; Kajiwara, Y.; Nakayama, H.; Yoshino, T.; Harii, K.; Fujikawa, Y.; Matsuo, M.; Maekawa, S.; Saitoh, E. Inverse spin-Hall effect induced by spin pumping in metallic system. J. Appl. Phys. 2011, 109, 103913.

(30) Azevedo, A.; Vilela-Leao, L. H.; Rodriguez-Suarez, R. L.; Santos, A. F. L.; Rezende, S. M. Spin pumping and anisotropic magnetoresistance voltages in magnetic bilayers: Theory and experiment. Phys. Rev. B 2011, 83, 144402.

Table 1. EMF values and the total charge current J_c calculated from the parallel circuit model for the Py/Pt device under pulse microwave irradiation (396 W).

Devices	$V_{emf,1M}$ *	$V_{emf,50}$ *	$V'_{emf,50}$ **	$J_{c,50}$ ***	$J_{c,1M}$ ***
Py/Pt	-10.22 mV	-4.04 mV	-3.80 mV	-1.3×10^2 μA	-1.2×10^2 μA

* $V_{emf,1M}$ and $V_{emf,50}$ indicate the EMF values obtained when the input resistance of the oscilloscope (R_L) is 1MΩ and 50Ω, respectively.

** $V'_{emf,50}$ is the EMF value at R_L = 50Ω calculated from $V_{emf,1M}$.

*** $J_{c,50}$ and $J_{c,1M}$ are the total charge current values calculated for R_L= 50Ω and 1MΩ, respectively using the relation of $J_{c,x} = V_{emf,x}(1/R_L+1/R_{pt})$ where x= 50 and 1M for R_L = 50Ω and 1MΩ, respectively. R_{pt} is the resistance measured from Pt terminals (84.5Ω) of the Py/Pt devices.

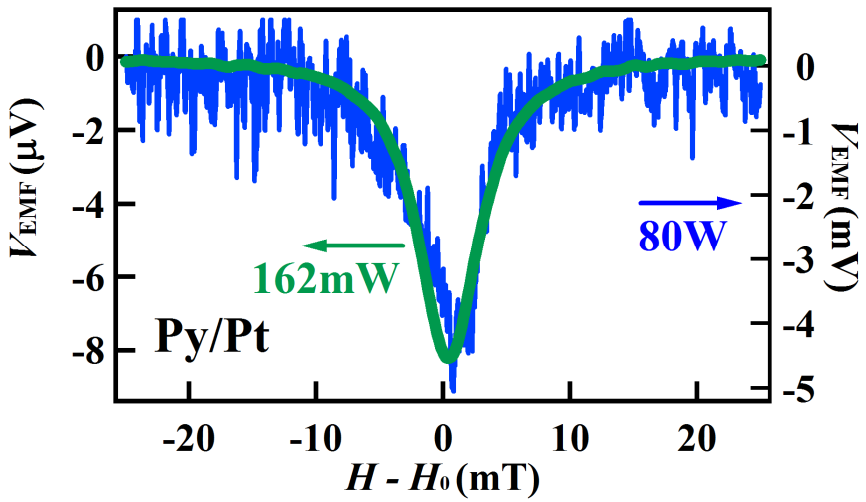

Figure 1. Comparison of the spectra of electromotive force (EMF) induced by ferromagnetic resonance (FMR) excitation of the permalloy (Py)/Pt device under the microwave irradiation of 162mW and 80W.

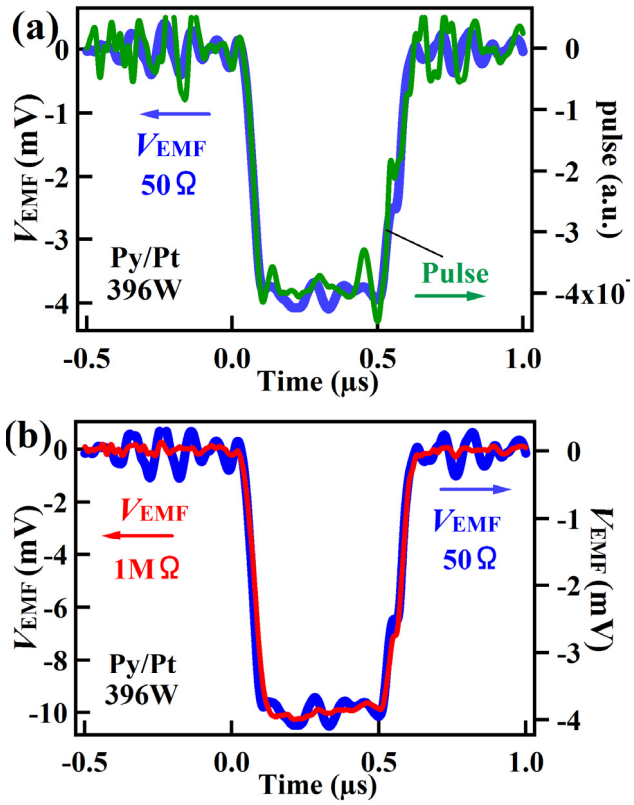

Figure 2. a. Comparison of the time-response waveforms of the EMF and microwave pulse (0.5 μs width). The EMF was measured at the peak magnetic field for a 396W-microwave pulse with the internal resistance (R_L) of 50Ω. **b** Comparison of the time-response waveforms of the EMF measured at the same peak field for the same pulse between R_L = 50 Ω and 1 MΩ.

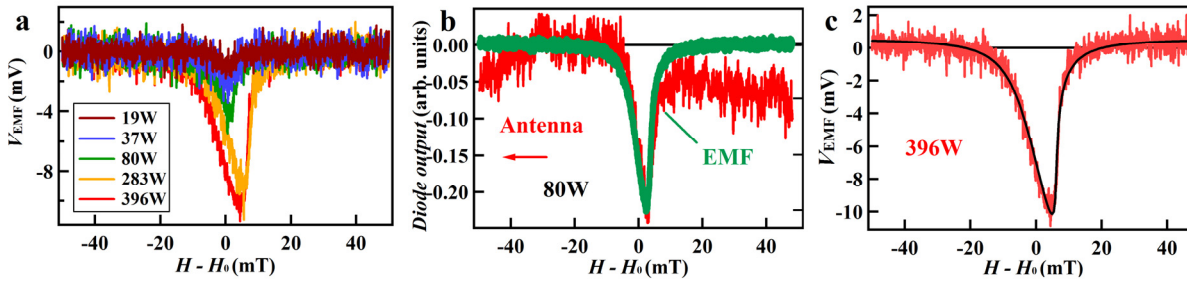

Figure 3. a. Microwave power dependence of EMF spectra under pulse microwave irradiation measured under R_L= 1MΩ. **b**. Comparison of the FMR spectrum during the pulse excitation under 80W-pulse irradiation obtained from the antenna probe measurement with the EMF spectrum measured simultaneously. **c**. Result of the spectral simulation using Eq. (1) for the EMF spectrum at 396W shown in **a**.

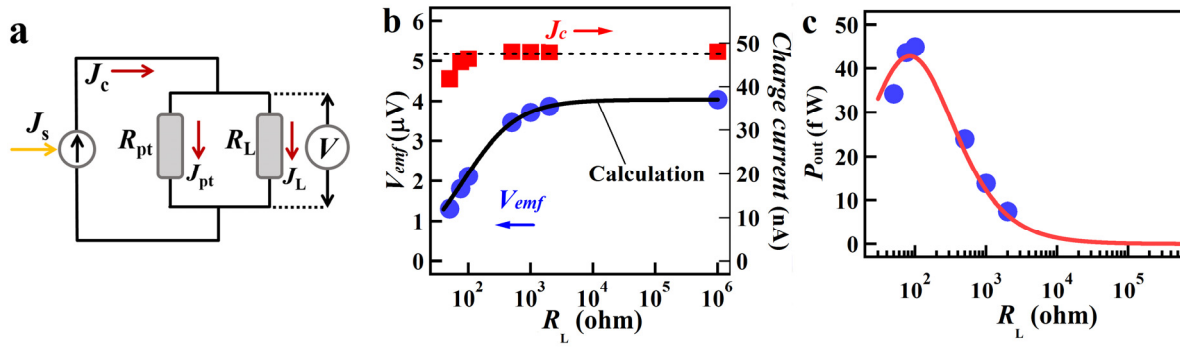

Figure 4. a Model of the parallel circuit consisting of the resistances of the external load (R_L) and Pt (R_{pt}). The charge currents (J_c) converted from spin current (J_s) flow in R_L and R_{pt} (J_L and J_{pt}, respectively) and the current ratio (J_L /J_{pt}) can be regulated by changing R_L. **b** The R_L-dependence of EMF measured for the Py/Pt device (V_{emf}) and the total charge current J_L+ J_{pt} (=J_c). The black solid curve in V_{emf} represents the prediction calculated from V_{emf} at R_{pt} =1MΩ. **c** The R_L-dependence of the output power at the external load P_{out} (top). The solid curve is the result of fit using Eq.(2).

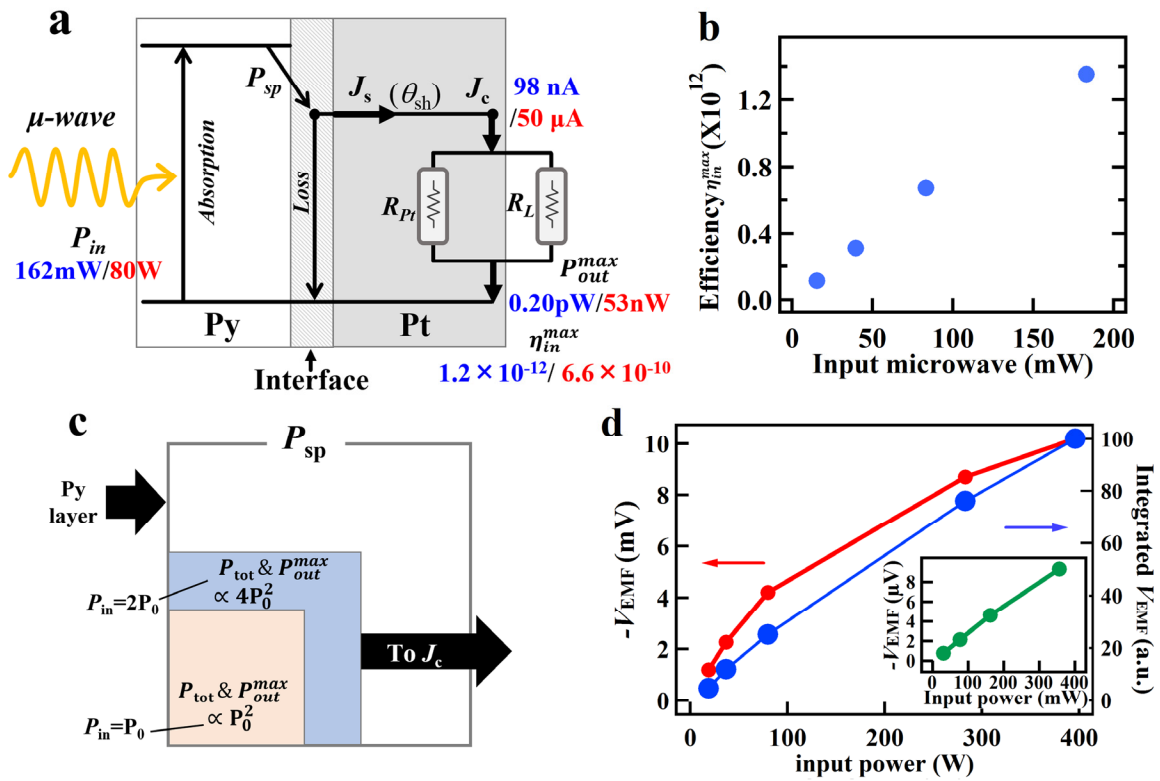

Figure 5. a Power flow chart of EMF-output by FMR-spin pumping for the Py/Pt device under 162mW and 80W microwave irradiations. η_{in}^{max} is the conversion efficiency of the power that can be maximally output (P_{out}^{max}) per the input microwave power (P_{in}). P_{sp} is the power injected from the Py-layer into the Pt layer. θ_{sh} is the spin Hall angle. **b** P_{in}–dependence of η_{in}^{max}. **c** Schematic representation of the proportion of the total power consumed inside the Pt layer and an external load (P_{tot}) to P_{sp} increasing with squared P_{in}: for instance, increasing P_i from P_0 to 2 P_0 doubles the ratio of P_{tot} to P_{sp}. **d** Input power dependence of V_{emf} peak values and spectral integrals in the spectrum of Fig. 3a. The inset shows the power dependence of V_{emf} below 200 mW.

SYNOPSIS (Word Style “SN_Synopsis_TOC”).